ELSEVIER

International Journal of Heat and Fluid Flow 21 (2000) 693–700

International Journal of HEAT AND FLUID FLOW

www.elsevier.com/locate/ijhff

Heat transfer to non-Newtonian flows over a cylinder in cross flow

B.K. Rao *

Heat Transfer Laboratory, Idaho State University, Campus Box 8362, Pocatello, ID 83209, USA

Received 23 December 1999; accepted 26 June 2000

Abstract

Over a range of $102 < Re^* < 5800$, $6.5 < Pr^* < 79$, and $0.6 < n < 1$, circumferential wall temperatures for water and aqueous polymer (purely viscous) solution flows over a smooth cylinder were measured experimentally. The cylinder was heated by passing direct electric current through it. Aqueous solutions of Carbopol 934 and EZ1 were used as power-law non-Newtonian fluids. The peripherally averaged heat transfer coefficient for purely viscous non-Newtonian fluids, at any fixed flow rate, decreases with increasing polymer concentration. A new correlation is proposed for predicting the peripherally averaged Nusselt number for power-law fluid flows over a heated cylinder in cross flow.

Keywords: Non-Newtonian; Heat transfer; Cross flow

1. Introduction

Heat transfer to Newtonian fluids from tubes of various cross-sections in cross flow has been extensively studied due to its applications in heat exchangers and hot-wire anemometry. The progress on this general topic has been reviewed by Žukauskas (1982). The heat transfer between a cylinder and a fluid in cross flow depends on the Reynolds number, the Prandtl number, surface roughness, free-stream turbulence intensity, heat flux direction (i.e. cooling or heating), thermal boundary condition, etc. For flows through confined spaces, the effects of aspect ratio, and several methods for correcting for solid and wake blockages have been summarized in review articles (Morgan, 1975; Žukauskas, 1972). The effect of surface roughness on augmented heat transfer from cylinders to Newtonian fluids in cross flow was reported by some research workers (Achenbach, 1977). The influence of free-stream turbulence intensity on laminar-turbulent boundary layer transition and on the average heat transfer for the cylinder in cross flow was reviewed by Kestin (1966).

Analytical solutions to heat transfer problem on the front part (from the stagnation point up to the separation of laminar boundary layer) are given by several authors (White, 1974; Kays and Crawford, 1980; Kakac and Yener, 1980). For circumferentially averaged heat transfer from a cylinder in cross flow, some well-known predictions, based on experimental results are:

$$Nu = ARe^m Pr^c (Pr_b/Pr_w)^a, \tag{1}$$

where a, A, m, and c are empirical constants which depend on the ranges of Re and Pr. Most of the experimental data in the literature for Newtonian flows suggest that the exponent c in Eq. (1) lies between 0.3 and 0.4.

$$Nu = (0.4Re^{1/2} + 0.06Re^{2/3})Pr^{0.4}(\mu_\infty/\mu_w)^{1/4} \tag{2}$$

for $0.7 \leqslant Pr \leqslant 300$, and $40 \leqslant Re \leqslant 10^5$ (Whitaker, 1972),

$$Nu = 0.3 + 0.62Re^{1/2}Pr^{1/3} \times [1 + (Re/282,000)^{5/8}]^{0.8}/[1 + (0.4/Pr)^{2/3}]^{1/4} \tag{3}$$

for $Re\ Pr \geqslant 0.2$ (Churchill and Bernstein, 1977). In Eq. (2), viscosity is evaluated at the wall temperature while all other physical properties are taken at the free-stream temperature. In Eq. (3), all properties are evaluated at the film temperature. Eq. (3) was developed based on experimental data of many investigators, and Newtonian fluids (air, water, and liquid metals) with both uniform wall temperature and uniform wall heat flux thermal boundary conditions.

Non-Newtonian fluids of several types such as Bingham plastics, dilatant, pseudoplastic, and viscoelastic fluids are used in many industries: petrochemical, pharmaceutical, biochemical, and food. The simplest mathematical model which describes the flow behavior of a power-law fluid is (Bird et al., 1960; Skelland, 1967):

$$\tau = K\dot{\gamma}^n = \eta\dot{\gamma}. \tag{4}$$

A few of the definitions of the Reynolds number cited in the literature on non-Newtonian flows are reviewed here. The apparent Reynolds number (Re_a) often used for power-law fluid flows through circular pipes is defined as (Metzner, 1965):

$$Re_a = \rho u D/\eta, \tag{5a}$$

where η is evaluated at $\dot{\gamma}$ corresponding to the measured wall shear stress. Kozicki et al. (1966) introduced a generalized Reynolds number (Re^*) such that the laminar isothermal

* Tel.: +1-208-282-2324; fax: +1-208-282-4538.
E-mail address: bk_rao@hotmail.com (B.K. Rao).

0142-727X/00/$ - see front matter
PII: S0142-727X(00)00063-1

Notation

A	cross-sectional area of flow passage at the entrance
c_p	test fluid specific heat
d	tube's inside diameter
D	tube's outside diameter
D_h	hydraulic diameter
h	heat transfer coefficient $= \dot{q}''/(T_{wo} - T_{bi})$
H	distance between the confining inner walls (of plexiglass chamber) parallel to the tube
I	electric current through the tube $= V_s/R_s$
k	thermal conductivity of test section wall
k_f	test fluid thermal conductivity
K	consistency index
L	heated length of the tube in contact with the fluid
n	power-law exponent
$\dot{q}''$	wall heat flux at the outside surface $= VI/(2\pi DL)$
$\dot{q}'''$	volumetric heat generation rate $= 4VI/[\pi L(D^2 - d^2)]$
$\dot{Q}$	measured volumetric flow rate of liquid
$\dot{Q}_e$	rate of electrical input $= VI$
$\dot{Q}_f$	rate of enthalpy gained by the fluid $= \rho Q c_p(T_{bo} - T_\infty)$
R_s	shunt resistance
Tu	turbulence intensity (%)
T_∞	fluid bulk temperature at the inlet = free-stream temperature
T_f	film temperature $= \frac{1}{2}(T_{wo} + T_\infty)$
T_{bo}	fluid bulk temperature at the outlet
T_{wi}	steel tube inner wall temperature
T_{wo}	steel tube outer wall temperature
u	fluid velocity adjusted for blockage effect $= U/(1 - D/H)$
U	reference velocity of test fluid $= Q/A$
V	adjusted voltage drop across the tube length inside the plexiglass chamber
V_s	voltage drop across the shunt

Dimensionless quantities

Gr	Grashof number $= g\beta(T_{wo} - T_\infty)D^3/\nu^2$
Nu	Nusselt number $= hD/k_f$
Nu_{ave}	peripherally averaged Nusselt number, Eq. (9c)
Pr	Prandtl number $= \mu c_p/k_f$
Pr_a	apparent Prandtl number $= \eta c_p/k_f$
Re	Reynolds number $= \rho uD/\mu$
Pr^*	$= Re_a Pr_a/Re^*$
Re_a	apparent Reynolds number, Eq. (5a)
Re^*	generalized Reynolds number, Eq. (5b)
Ra	Rayleigh number $= GrPr^*$

Greeks

β	volumetric coefficient of expansion
$\dot{\gamma}$	shear rate of viscometric flow
η	apparent viscosity of power-law fluid
θ	angle measured from stagnation point
μ	dynamic viscosity of Newtonian fluid
ν	kinematic viscosity $= \eta/\rho$
ρ	test fluid density

Subscripts

a	based on apparent viscosity
ave	peripherally averaged
b	bulk temperature
f	film temperature
m	measured
p	predicted
w	at the test section wall

Fanning friction factor for fully developed flow through any channel of arbitrary but uniform cross-section is given by $f = 16/Re^*$ where

$$Re^* = \rho u^{2-n} D_h^n / \{K[(3n+1)/4n]^n 8^{n-1}\}. \quad (5b)$$

Some of the available experimental data on friction factor and heat transfer behavior of power-law fluid turbulent flows through channels were better correlated in terms of Re^* (Rao, 1994) while those for viscoelastic fluids were often expressed in terms of Re_a (Rao, 1993). For Newtonian fluids ($n = 1$), both Re_a and Re^* reduce to Re.

An excellent review article (Shenoy and Mashelkar, 1982) dealt with analytical studies on *free* convection heat transfer to non-Newtonian fluids from different geometries. Limited *experimental* results were reported on *forced* convection heat transfer to power-law flows over a cylinder (Luikov et al., 1969; Mizushina et al., 1978; Shah et al., 1962).

The heat exchanger designers are often interested in estimating the average Nusselt value using correlations based on easily obtainable viscometric properties. The objective of the present *experimental* investigation is to develop a simple *and* reliable prediction for the peripherally averaged *forced* convection heat transfer to power-law fluids from a heated cylinder in cross flow.

2. Experimental apparatus and procedure

The flow loop schematic is shown in Fig. 1. A 14 cm long, 24.3 mm (±0.3%) OD, type-316 stainless steel tube was symmetrically placed horizontally at the mid-section of a plexiglass chamber (with inside dimensions 5 cm × 7.5 cm and 0.3-m high) of 6.35 mm wall thickness such that the cylinder length inside the chamber was 7.5 cm. The tube was precision bored on the inside and was machined on the outside to achieve a surface finish of 2.54 μm and the wall thickness of 0.6 mm (±0.25%). Some 12 thermocouples were mounted on the inner

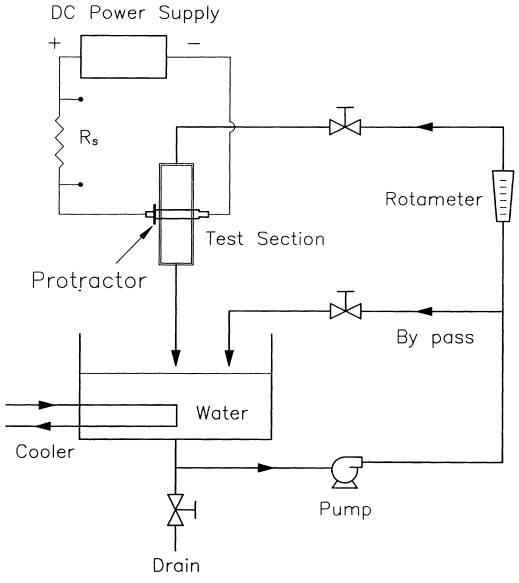

Fig. 1. Schematic of flow loop.

surface of the tube, using copper oxide cement and a commercial resin, at three sections (see Fig. 2) along the isotherms. A hollow teflon tube was slit (longitudinally) into two halves and inserted into the steel tube to press against the inner walls of the latter by means of four compression springs placed at an interval of 25 mm measured along the tube axis. All thermocouples had excellent thermal contact with the test section. The thermocouple wires were routed through the interior of the steel tube and brought out at one end of it, and at the other end a protractor was mounted (within 1 mm from the plexiglass outer wall) to measure the angular position (θ) of the thermocouples relative to the stagnation point. These thermocouples, mounted on the tube inner surface, were calibrated (against a platinum-resistance thermometer) over a temperature range from 10°C to 60°C. The thermocouple output (emf) was linear within this range of the temperature. The teflon tube interior was filled with fiber-glass wool to provide insulated thermal boundary condition.

The cylinder was rotated at 11.25° intervals from $\theta = 0°$ (at forward stagnation point) to 180°. The variation in the output (mV) of all thermocouples (attached to the tube), when positioned at any given θ, was <1%. These thermocouples provided a check on the flow symmetry. A flow transition piece was provided upstream of the test section (connecting it with the 38.1 mm ID tube) to achieve uniform velocity at its entrance. A mixing chamber (38.1 mm ID and 0.15 m long) was attached at the test section downstream (not shown in Fig. 1). Thermocouples for fluid bulk temperature measurement were placed inside the reservoir and in the mixing chamber. All thermocouples used here were of *T*-type (copper–constantan), gage 30.

A DC power supply (0–12 V, 0–400 A) was used to heat the steel tube. On either end of the steel tube which protruded from the plexiglass chamber, detachable steel end-connectors were mounted into which the power supply cables could be inserted. Silver wires were soldered on the protruding part of the steel tube on either side of the plexiglass chamber, close to its outer walls. The measured voltage drop across the soldered junctions (of known distance apart) was reduced in direct proportion to the length of the steel tube inside the plexiglass chamber (V). A precision resistor was connected in series with the power supply and the steel tube. From the voltage drop across the precision resistor (V_s) and the known resistance (R_s), the current through the tube was obtained.

The non-Newtonian test fluids, in this study, were aqueous solutions of Carbopol 934® (at concentrations of 250, and 500 ppm by weight) and Carbopol EZ1® (at 500 ppm). The rheology of polymer solutions is sensitive to solvent chemistry (Cho and Hartnett, 1982). In light of this, for better reproducibility of results, distilled water was used as solvent. The test fluid was prepared in the reservoir at 20°C. In order to achieve lower values of n, and to minimize the surface contamination, the Carbopol solutions were neutralized with sodium hydroxide solution (10% strength) until the pH reached an *optimal* value ≈7.2 (Rao, 1994). The rheology of polymer solutions is sensitive to mechanical degradation (Walters, 1975). To minimize mechanical degradation of the polymer, a positive displacement pump with a variable-speed drive was used; only hand-stirring was employed to dissolve the polymer in water. To make sure that biological degradation of the polymer was minimal, a fresh batch of solution was prepared for each run and was dispensed immediately. The temperature of test fluid in the reservoir was maintained at 20 ± 0.1°C by manually adjusting the water flow rate through the immersed cooling coil.

Each run with polymer solution was repeated three times and the variation in the average *Nu* was within ±3%. After every three consecutive runs with polymer solution, the steel tube was removed from its housing for visual inspection of the surface condition, and was cleaned. After reinstalling the tube, heat transfer was measured for distilled water flow to ensure the cleanliness of test section surface. This cumbersome procedure was essential since Carbopol solutions, like most other power-law fluids, foul the surfaces (especially at hot spots) they come in contact with. To re-establish this well-known *fouling* effect, heat transfer to water was measured immediately following about six or seven runs in a row with Carbopol 934 solutions. The average Nu for water runs with the contaminated tube was up to 35% lower than that with the clean tube. Similar observations were made with Carbopol EZ1 500 ppm solutions as well. By trial, it was found that the maximum number of Carbopol runs in a row (before the tube has to be cleaned) was three.

The cylinder was heated by passing direct electric current through it which yielded uniform wall heat flux thermal boundary condition. The maximum current passed through the test section was 335 A and the corresponding voltage drop across the tube (adjusted for its length inside the plexiglass chamber) was about 0.32 V. The fluctuation of voltage across

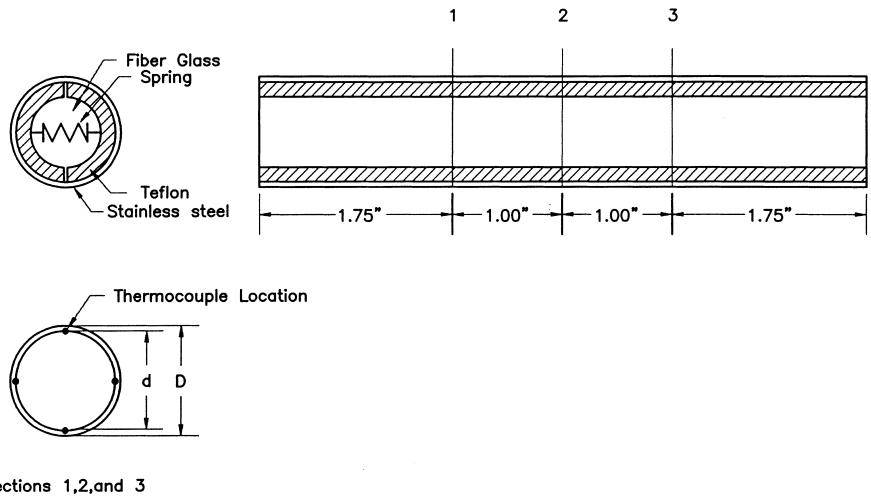

Fig. 2. Details of the test section.

the heated tube was within ±0.5%. With the computer-controlled pump drive, the flow rate oscillation was kept within ±1%. The rotameter reading was monitored by measuring the flow rate with a stop watch and bucketing the fluid exiting the test section.

The volumetric flow rate was noted manually. All electrical outputs (thermocouple readings, voltage drop across the tube and the shunt) were logged in with a data acquisition system, after the thermal equilibrium was reached. Typically, it would take about 35 min before such a steady state was reached.

For aqueous polymer solutions studied all the physical properties (except viscosity) were taken to be the same as for water (Lee et al., 1981). The test fluid rheology (τ as a function of $\dot{\gamma}$) was measured using a Brookfield viscometer, and a Bohlin rheogoniometer at different temperatures ranging from 15°C to 55°C and a parabolic equation was fitted:

$$\ln\ \tau = a_0 + a_1[\ln\dot{\gamma}] + a_2[\ln\dot{\gamma}]^2. \tag{6}$$

The rheological constants and η were, then, calculated:

$$n = \mathrm{d}[\ln\tau]/\mathrm{d}[\ln\dot{\gamma}] = a_1 + 2a_2[\ln\dot{\gamma}], \tag{7a}$$

$$K = \exp[a_0 - a_2(\ln\dot{\gamma})^2], \tag{7b}$$

$$\eta = \tau/\dot{\gamma}. \tag{7c}$$

The characteristic curves (η as a function of $\dot{\gamma}$, at 20°C) are shown in Fig. 3. A temperature correction was applied for viscosity. To monitor the polymer degradation, the test fluid rheology was measured (at 20°C) before and after each run and the variation was found to be within ±2%.

3. Results and discussion

The energy balance was monitored for all runs by comparing the rate of electrical energy input ($\dot{q}_e$) with the rate of enthalpy gained by the test fluid ($\dot{q}_f$). $\dot{q}_e$ was always more than $\dot{q}_f$ and the deviation was <2% for all the experimental runs here. The maximum values of the Grashof number, *Gr*, and the Rayleigh number, *Ra*, for all the runs in this study were less than 0.8×10^6 and 7×10^7, respectively. Also, the quantity Gr/Re^2 was $\ll 1$ for all the runs reported here, suggesting that the effect of free convection on the measured *Nu* is insignificant (Chen and Armaly, 1987; Hatton et al., 1970; Van der Hegge and Zijnen, 1956).

At any given θ, the readings of the thermocouples at all three sections (aligned parallel to the tube axis, but at the same θ) were within 1% of their average. This suggests that the axial conduction was negligible at least in the mid two-thirds of the cylinder length. The outer wall temperature was estimated, with the justification above, solving the one-dimensional steady state heat conduction equation:

$$T_{wo} = T_{wi} - (\dot{q}'''/16k)[D^2 - d^2 + 2d^2\ln(d/D)]. \tag{8}$$

The estimated outer wall circumferential temperature profiles for typical runs are shown in Fig. 4. Exact analysis for the tube outer wall temperature requires solving the conjugate problem. An approximate analysis was made for a conservative estimate of the circumferential heat conduction. The annular cross-section of the tube was divided into 32 equal parts and an energy balance was made on each cell using the measured inner wall temperature and internal heat generation. The maximum contribution from circumferential heat conduction was <0.6% of the volumetric heat generation for all runs reported here.

The experimental data presented here were obtained for liquid flow in the direction of gravity. For the local *Nu* calculations, the test fluid properties were evaluated at T_f whereas for Re^* and Pr^*, the liquid properties were taken at T_∞.

Several methods for correcting solid and wake blockage effects have been suggested (Perkins and Leppert, 1962; Knudsen and Katz, 1958; Robinson et al., 1951), but these methods differ appreciably. The approach due to Mikheyev (1968) was used here to adjust the fluid velocity (U) at the plexiglass chamber inlet for blockage (D/H) effect. For non-Newtonian fluids, η, K, and n (all depend on $\dot{\gamma}$) vary around the cylinder. Despite some controversy, a voluminous body of literature uses viscometric data for some non-viscometric steady flows (such as those through confined spaces in compact heat exchangers) for simplifying the design calculations (Schowalter, 1977). In this study, the adjusted velocity (u), and reference shear rate, $\dot{\gamma} = 2u/D$, were used, for data reduction, while a few other (some what *arbitrary*) choices are available (Mizushina et al., 1978; Shah et al., 1962).

The measured local Nusselt numbers for typical runs are shown in Fig. 5, from which it can be seen that for water, a Newtonian fluid, *Nu* exhibited two minima around the cylinder (for $3300 < Re < 5800$). This is the *critical* flow regime. The first minimum occurred at the laminar to turbulent transition of the boundary layer; the second minimum occurred at the flow separation point. The respective values of θ for these

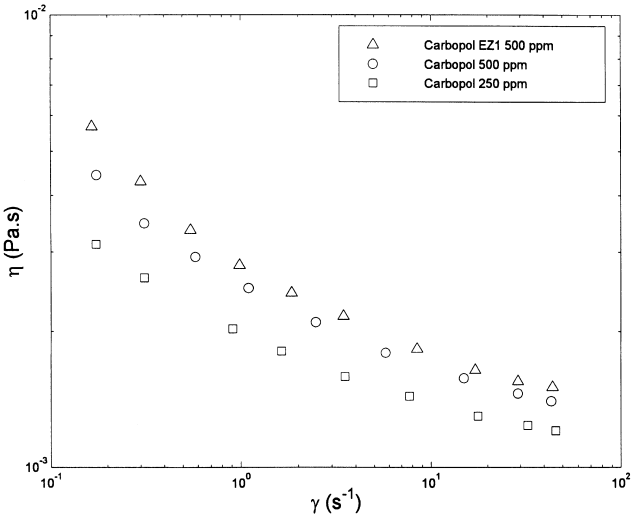

Fig. 3. Characteristic curves for Carbopol solutions.

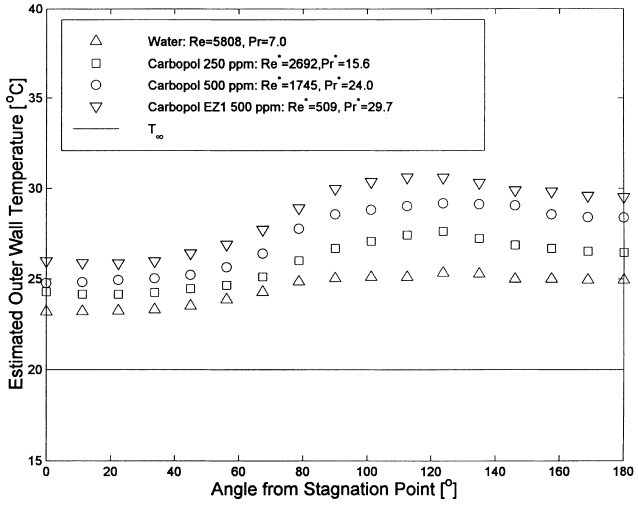

Fig. 4. Wall temperature distribution for typical runs.

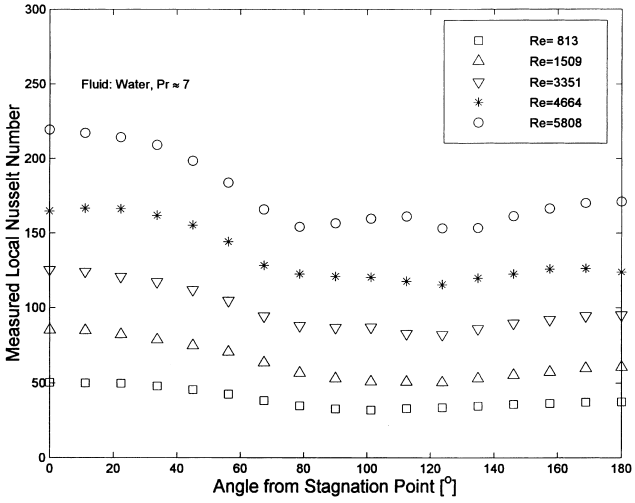

Fig. 5. Measured local Nusselt number versus angle for typical runs with water.

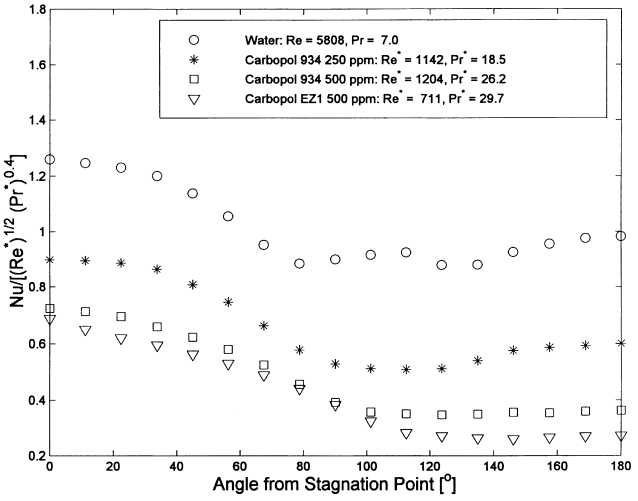

Fig. 7. $Nu/[(Re^*)^{1/2}(Pr^*)^{0.4}]$ versus angle for typical runs.

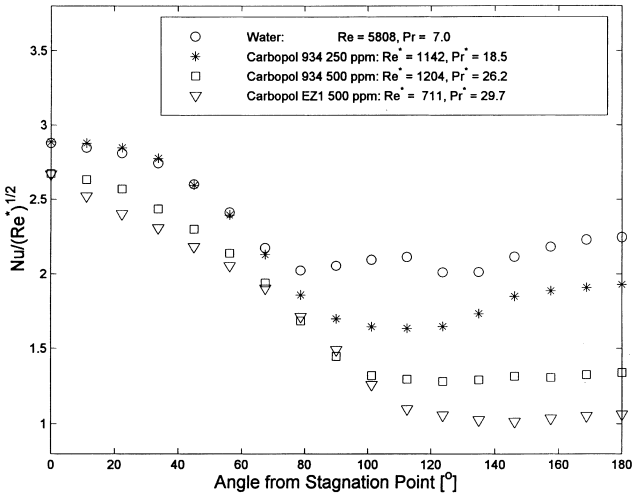

Fig. 6. $Nu/(Re^*)^{1/2}$ versus angle for typical runs.

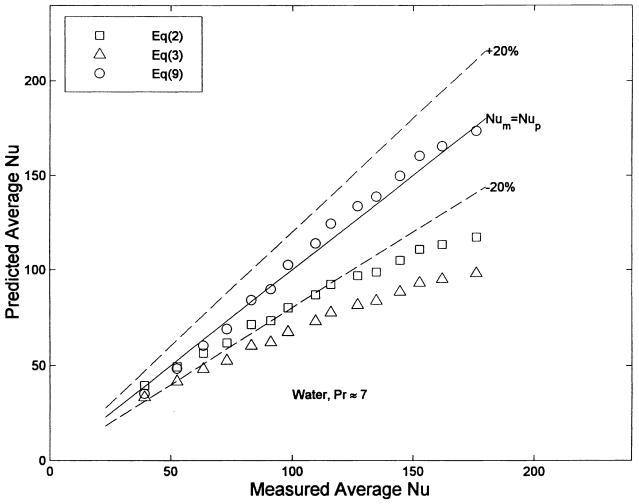

Fig. 8. Predicted *Nu* versus measured *Nu* for water.

minima of *Nu* were in agreement with those reported in the literature (Giedt, 1949; Žukauskas, 1972). No *separation bubble* was noticed here at the location for first minimum of *Nu* unlike in some published results (ukauskas, 1982). For $Re < 2700$, only one minimum in the variation of *Nu* around the cylinder was noticed for water runs in this study (Eckert and Soehngen, 1952). This is the *subcritical* regime in which *Nu* at the front stagnation point is at its maximum and it decreases as the laminar boundary layer develops. If the *Re* were large enough, then, the *Nu* would gradually increase past the laminar boundary layer separation.

In Fig. 6, the quantity $Nu/(Re^*)^{1/2}$ is shown as a function of θ. Some experimental studies (Žukauskas, 1987) suggest that the critical flow regime is reached when $Re\ Tu > 150,000$. From Fig. 6, it is apparent that the water data (at $Re = 5800$) are in the critical regime. No quantitative comparison of the present data with those in the literature was possible since the turbulence intensity was not measured in this study.

In Fig. 7, the quantity $Nu/[(Re^*)^{1/2}(Pr^*)^{0.4}]$ is shown as a function of θ. From Figs. 5–7, it can be seen that the present results for Carbopol solutions are in the subcritical regime. It should be noted that aqueous polymer solutions become quite viscous (as the polymer concentration is increased) and therefore, delay the laminar to turbulent transition and suppress turbulence intensity. In order to reach the critical regime, much higher flow rates are required. The capacity of the positive displacement pump used here set the limit for the highest concentration and the maximum flow rate (500 ppm, and 5.1×10^{-4} m^3/s) used in this study.

In Fig. 8, the measured peripherally averaged *Nu* for water are compared with those yielded by some of the available predictions. Both Eqs. (2) and (3) under-predicted the present experimental *Nu* for water, over the range $813 \leqslant Re \leqslant 5808$. This deviation is attributed to the relatively high blockage ratio ($D/H = 0.479$) in this study.

The measured *local Nu* for typical runs of Carbopol solutions are shown in Figs. 9 and 10 from which it can be seen that the *Nu* decreases with increasing polymer concentration (hence, decreasing *n* and increasing Pr^*), at any given Re^*. This observed behavior of power-law fluids is contrary to that in internal flows in which the *Nu* increases with decreasing *n*, at any fixed flow rate (Rao, 1994).

The present experimental results for Carbopol solutions could not be compared with those in the literature, due to

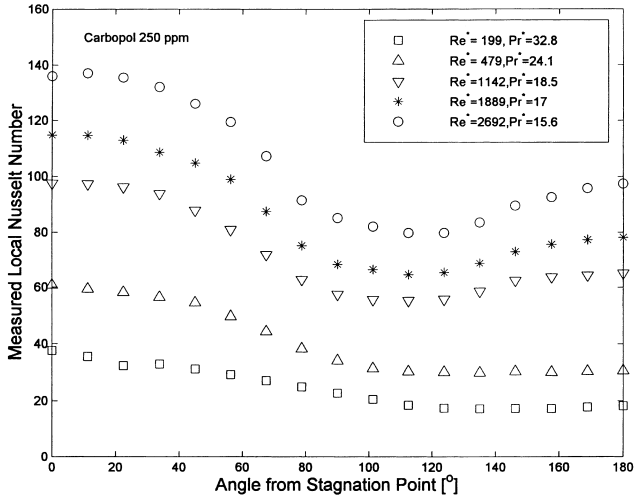

Fig. 9. Measured local Nusselt number versus angle for typical runs with Carbopol solutions.

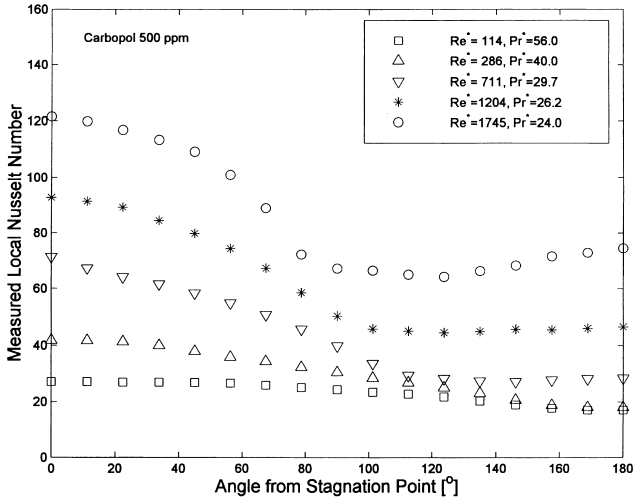

Fig. 10. Measured local Nusselt number versus angle for typical runs with Carbopol solutions.

significant differences in the experimental conditions. Shah et al. (1962) presented the local Nusselt number for mildly viscoelastic flows in the region near forward stagnation point. Mizushina and Usui (1978) reported their numerical solution for the heat transfer near the stagnation region of a cylinder in a viscoelastic cross flow. Shah et al. (1962) and Mizushina et al. (1978) used $\dot{\gamma} = 4U/D$ in their analysis on power-law flows over a cylinder. The definitions of the Reynolds number and the Prandtl number reported by Shah et al. (1962) and Mizushina et al. (1978) are different from those used here. The blockage ratio in this investigation and the ones reported by Shah et al. (1962) and Mizushina et al. (1978) are 0.479, 0.25, and 0.083, respectively. Shah et al. (1962) did not impose uniform heat flux thermal boundary condition. The effect of fouling on heat transfer to power-law fluids was not reported in the literature. The measurement uncertainties cited in the literature varied considerably. Some investigators failed to mention the errors in temperature measurement if the thermocouples were not laid out along the isotherms.

The predicted average *Nu* for power-law fluids using the Newtonian correlations (Eqs. (2) and (3)) are graphically

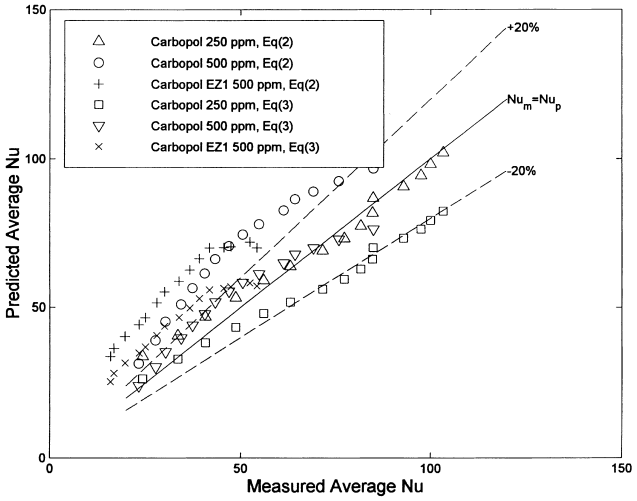

Fig. 11. Predicted *Nu* versus measured *Nu* for Carbopol solutions.

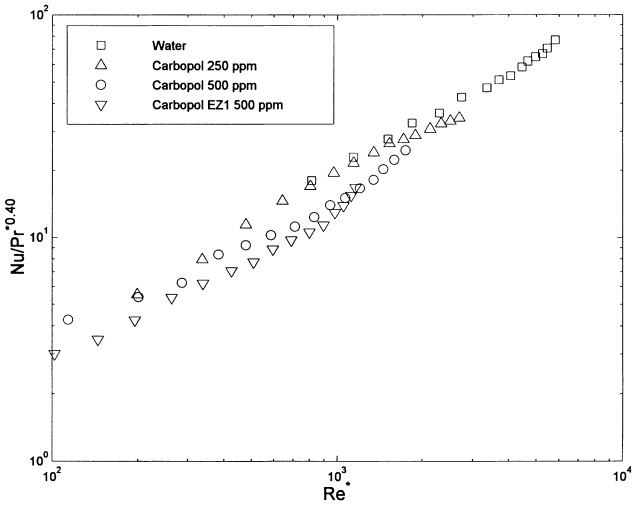

Fig. 12. $Nu/(Pr^*)^{0.4}$ versus Re^* for water and Carbopol solutions.

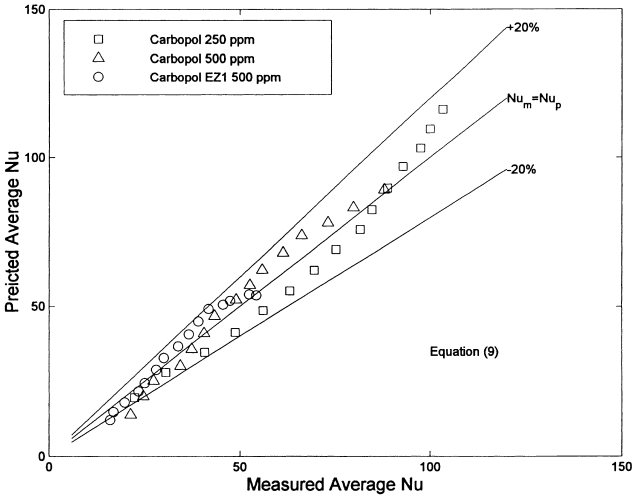

Fig. 13. Predicted *Nu* versus measured *Nu* for Carbopol solutions.

Table 1
Range of parameters

Fluid		Re^*	Pr^*	n
Water		813–5800	6.5–8.2	1.0
Carbopol	934 250 wppm	205–3538	20.9–42.8	0.71–0.76
	500 wppm	120–2280	34.4–65.0	0.64–0.69
	EZ1 500 wppm	102–1092	36.1–78.9	0.60–0.65

shown in Fig. 11. It can be seen from Fig. 11 that Eq. (2) over-predicts while Eq. (3) under-predicts the present data. In Fig. 12, the quantity $Nu/(Pr^*)^{0.4}$ is shown as a function of Re^* for water and Carbopol solutions. From Fig. 12 it can be seen that the quantity $Nu/(Pr^*)^{0.4}$ has some *explicit* dependency on n over the range $0.6 \leqslant n \leqslant 1$, and $102 \leqslant Re^* \leqslant 5800$.

Based on the present experimental results, the following *new* and *simple* correlation is proposed for peripherally averaged heat transfer to power-law fluid from a heated smooth cylinder with uniform heat flux, in cross flow:

$$Nu_{\text{ave}} = f(n)\ (0.165Re^{0.15} + 0.079\ Re^{0.79})Pr^{g(n)}(\mu_\infty/\mu_w)^{0.25}, \quad (9)$$

$$f(n) = -2.24 + 7.17n - 3.93n^2, \quad (9a)$$

$$g(n) = 0.4 + 0.05(1-n), \quad (9b)$$

where

$$Nu_{\text{ave}} = \int_0^\pi Nu(\theta)\ \mathrm{d}\theta/\pi \quad (9c)$$

with validity over the range: $102 \leqslant Re^* \leqslant 9600,\ 6.5 \leqslant Pr^* \leqslant 79$, and $0.60 \leqslant n \leqslant 1.0$. The constants in Eqs. (9a) and (9b)) were obtained from regression analysis.

From Fig. 13 it can be seen that the present experimental *peripherally averaged Nu* values for water as well as for power-law fluids are in good agreement with the predicted using Eq. (9), within the range of the parameters here (see Table 1).

The estimated uncertainties, using the root-sum-square method, in the Re^* and the Nu are $\pm 4.7\%$ and $\pm 6.1\%$, respectively.

4. Conclusions

1. Heat transfer to purely viscous power-law fluids from a hot cylinder decreases, with decreasing n value, at any given Re^*.
2. At higher concentrations of polymer, Nusselt number variation with θ has only one minimum.
3. Heat transfer to purely viscous power-law fluids, within the range: $102 \leqslant Re^* \leqslant 5800,\ 6.5 \leqslant Pr^* \leqslant 79$, and $0.6 \leqslant n \leqslant 1$ can be predicted accurately using Eq. (9).

5. Recommendations

More data with other polymers are needed to develop generalized correlations for non-Newtonian forced convection heat transfer in cross flow. The empirical constants, and exponents in Eq. (9) depend on the ranges of Re^* and Pr^* (which in turn depend on the reference $\dot{\gamma}$) and the temperature at which the thermophysical properties would be taken. Attempts may be directed towards measuring velocity profiles for power-law fluid flows around a cylinder where temperature and $\dot{\gamma}$ change rapidly. Although designers prefer simple correlations (without compromising accuracy) and a convenient choice of η (in complex flow fields such as the case here), predictions based on Re^*, Pr^*, etc estimated at η obtained from detailed velocity field will form a very useful theoretical basis and help in a better understanding of the problem. Fouling effects on the heat transfer surfaces exposed to power-law fluids need be addressed thoroughly.

Acknowledgements

This research was in part funded by J. R. Simplot Co. and Ash Grove Cement Co.

References

Achenbach, E., 1977. The effect of surface roughness on the heat transfer from a circular cylinder to the cross flow of air. Int. J. Heat Mass Transfer 20, 359–369.

Bird, R.B., Armstrong, R.C., Hassager, O., 1960. Dynamics of Polymeric Liquids, vol. 1. Wiley, New York.

Chen, T.S., Armaly, B.F., 1987. Mixed convection in external flow. In: Kakaç, S., Shah, R.K., Aung, W. (Eds.), Handbook of Single-Phase Convective Heat Transfer. Wiley, New York.

Cho, Y.I., Hartnett, J.P., 1982. Non-Newtonian fluids in circular pipe flow. Adv. Heat Transfer 15, 59–141.

Churchill, S.W., Bernstein, M., 1977. A correlating equation for forced convection from gases and liquids to a circular cylinder in cross flow. J. Heat Transfer 99, 300–306.

Eckert, E.R.G., Soehngen, E., 1952. Distributions of heat-transfer coefficients around circular cylinders in cross flow at reynolds numbers from 20 to 500. Trans. ASME 74, 343–347.

Giedt, W.H., 1949. Investigation of variation of point unit heat transfer coefficient around a cylinder normal to an air stream. ASME Trans. 71, 375–381.

Hatton, A.P., James, D.D., Swise, H.W., 1970. Combined forced and natural convection with low-speed air flow over horizontal cylinders. J. Fluid Mech. 42, 15–31.

Kakac, S., Yener, Y., 1980. Convective Heat Transfer, Hemisphere, New York, p. 512.

Kays, W.M., Crawford, M.E., 1980. Convective Heat and Mass Transfer. McGraw-Hill, New York.

Kestin, J., 1966. The effect of free-stream turbulence on heat transfer rates. Adv. Heat Transfer 3, 1–32.

Knudsen, J.G., Katz, D.L., 1958. Fluid Dynamics and Heat Transfer. McGraw-Hill, New York.

Kozicki, W., Chou, C.H., Tiu, C., 1966. Non-Newtonian flow in ducts of arbitrary cross-sectional shape. Chem. Eng. Sci. 21, 665–679.

Lee, W.Y., Cho, Y.I., Hartnett, J.P., 1981. Thermal conductivity measurements of non-Newtonian fluids. Lett. Heat Mass Trans. 8, 255–259.

Luikov, A.V., Shulman, Z.P., Puris, B.I., Zhdanovich, N.V., 1969. Prog. Heat Mass Transfer 2.

Metzner, A.B., 1965. Heat transfer in non-Newtonian fluids. Adv. Heat Transfer 2, 357–397.

Mikheyev, M.A., 1968. Fundamentals of Heat Transfer, second ed.. Peace Publishers, Moscow English translation.

Mizushina, T., Usui, H., 1978. Approximate solution of the boundary layer equations for the flow of a non-Newtonian fluid around a circular cylinder. Heat Transfer Jpn. Res. 7 (2), 83–92.

Mizushina, T., Usui, H., Veno, K., Kato, T., 1978. Experiments of pseudoplastic fluid cross flow around a circular cylinder. Heat Transfer Jpn. Res. 7 (3), 92–101.

Morgan, V.T., 1975. The overall convective heat transfer from smooth circular cylinders. Adv. Heat Transfer 11, 199–264.

Perkins, H.C., Leppert, G., 1962. Forced convection heat transfer from a uniformly heated cylinder. J. Heat Trans. 80, 257–263.

Rao, B.K., 1993. Turbulent heat transfer to viscoelastic fluids in helical passages. Exp. Heat Transfer 6, 189–203.

Rao, B.K., 1994. Turbulent heat transfer to power-law fluids in helical passages. Int. J. Heat Fluid Flow 15 (2), 142–148.

Robinson, W., Han. L.S., Essig, R.H., Heddleson, C.F., 1951. Heat transfer and pressure drop data for circular cylinders in ducts and various arrangements. Report 41, Ohio State University Research Foundation, Columbus, OH.

Schowalter, W., 1977. Mechanics of Non-Newtonian Fluids. Pergamon, Oxford.

Shah, M.J., Petersen, E.E., Acrivos, A., 1962. Heat transfer from a cylinder to a power-law non-Newtonian fluid. AIChEJ 8 (4), 542–549.

Shenoy, A.V., Mashelkar, R.A., 1982. Thermal convection in non-Newtonian fluids. Adv. Heat Transfer 15, 143–225.

Skelland, A.H.P., 1967. Non-Newtonian Flow and Heat Transfer. Wiley, New York.

Van der Hegge, Zijnen, B.G., 1956. Modified correlation formulae for the heat transfer by forced convection from horizontal cylinders. Appl. Sci. Res. Ser. A 6, 129–140.

Walters, K., 1975. Rheometry. Wiley, New York.

Whitaker, S., 1972. Forced convection heat transfer calculations for flow in pipes, past flat plates, single cylinders, and for flow in packed beds and tube bundles. AIChEJ 18, 361–371.

White, F.M., 1974. Viscous Fluid Flow. McGraw-Hill, New York.

Žukauskas, A., 1972. Heat transfer from tubes in crossflow. Adv. Heat Transfer 8, 93–160.

Žukauskas, A., 1982. Konvektivnyi perenos v Teploobmennikakh, (Convective Transfer in Heat Exchangers) Nauka, Moscow.

Žukauskas, A., 1987. Convective heat transfer in cross flow. In: Kakac, S., Shah, R.K., Aung, W. (Eds.), Handbook of Single-Phase Convective Heat Transfer. Wiley, New York.